The Astrophysical Journal Letters, 724:L143–L147, 2010 December 1 doi:10.1088/2041-8205/724/2/L143

THE FIRST BENT DOUBLE LOBE RADIO SOURCE IN A KNOWN CLUSTER FILAMENT: CONSTRAINTS ON THE INTRAFILAMENT MEDIUM

Louise O. V. Edwards[1], Dario Fadda[1], and David T. Frayer[2]
[1] NASA Herschel Science Center, Caltech 100-22, Pasadena, CA 91125, USA; louise@ipac.caltech.edu
[2] NRAO, Green Bank, WV 24944, USA
Received 2010 September 1; accepted 2010 October 20; published 2010 November 8

ABSTRACT

We announce the first discovery of a bent double lobe radio source (DLRS) in a known cluster filament. The bent DLRS is found at a distance of 3.4 Mpc from the center of the rich galaxy cluster, A1763. We derive a bend angle $\alpha = 25^\circ$, and infer that the source is most likely seen at a viewing angle of $\Phi = 10^\circ$. From measuring the flux in the jet between the core and further lobe and assuming a spectral index of 1, we calculate the minimum pressure in the jet, $(8.0 \pm 3.2) \times 10^{-13}$ dyn cm^{-2}, and derive constraints on the intrafilament medium (IFM) assuming the bend of the jet is due to ram pressure. We constrain the IFM to be between (1–20) $\times 10^{-29}$ gm cm^{-3}. This is consistent with recent direct probes of the IFM and theoretical models. These observations justify future searches for bent double lobe radio sources located several megaparsecs from cluster cores, as they may be good markers of super cluster filaments.

Key words: galaxies: clusters: individual (A1763, A1770) – galaxies: clusters: intracluster medium – large-scale structure of universe – radio continuum: galaxies

1. INTRODUCTION

Bent double lobe radio sources (DLRSs) are rare, found in only 6% of clusters (Blanton et al. 2001). The bend is thought to be caused by ram pressure of the host cluster or group medium (Owen & Rudnick 1976), by an interaction with the host galaxy, or by merger activity with another galaxy (Rector et al. 1995). The environment surrounding a bent DLRS has been considered for decades (Kundt & Gopal-Krishna 1980; Gower & Hutchings 1984; Blanton 2000; de Vries et al. 2006). However, this only includes a region out to the virial radius of the system, most often an intermediate density group (Croston 2008; Zirbel 1997). Cluster scale filaments are also postulated to be host to bent DLRSs (Freeland et al. 2008), but the classification of such structures is observationally difficult as the galaxy density is low and the physical scale on the sky is vast.

We have been studying the super structure comprised of the rich cluster A1763 and the poor cluster A1770. A filament which connects the two was discovered using mid-IR observations from the *Spitzer Space Telescope* (Fadda et al. 2008), confirmed by collecting hundreds of member galaxy redshifts, and observed in 13 optical and IR bands (Edwards et al. 2010a). With new Very Large Array (VLA) data (Edwards et al. 2010b) we have discovered a DLRS (F1) located in the cluster feeding filament, well beyond the virial radius.

We announce this first detection of a bent DLRS in a known cluster filament. We use the properties of the bend to constrain the density of the surrounding intrafilament medium (IFM). We adopt a cosmology with $\Omega_m = 0.3$, $\Omega_\Lambda = 0.7$, and $H_o = 70$ km s^{-1} Mpc^{-1}, where one arcsec corresponds to 3.7 kpc at a redshift of 0.23.

2. OBSERVATIONS AND DATA REDUCTION

The data reduction for the VLA 1.4 GHz maps is discussed in detail in the companion paper, Edwards et al. (2010b). Both the FIRST survey (rms = 120 μJy beam^{-1}) and NVSS (rms = 450 μJy beam^{-1}) detect this source as an unresolved point at 1.4 GHz. We achieve a spatial resolution of 5 arcsec, and in our deeper observations (rms = 28 μJy beam^{-1}) two diffuse lobes on either side of the point source appear.

3. RESULTS

3.1. Physical Properties of the Source

The physical location of the DLRS, named F1 in Edwards et al. (2010b), is at $13^h36^m36^s.6$ $+41^d04^m34^s.7$ (J2000). Figure 1 (left) shows the relative distance of F1, $\sim$15.′3 (3.4 Mpc) from A1763's brightest cluster galaxy, well outside the virial radius of either cluster and along the galaxy filament.

F1 is a radio galaxy with a 1.4 GHz power of 9.6×10^{23} W Hz^{-1}. The flux is dominated by an unresolved core and includes two diffuse lobes which have an intensity ratio of 2.25, clearly visible in Figure 2. The lobe closest to the core is not only brighter, but also more compact than the elongated further lobe. We measure the core–lobe distance $l_1 = 12.''5$ (171 kpc), and the lobe distance ratio to be 3.55. Based on the FRI/FRII power break (Ledlow & Owen 1996), and the fact that the source is core dominated (Fanaroff & Riley 1974), we classify F1 as an FRI.

As the two lobes are aligned, the source is probably nearly along the line of sight. However, as part of the jet does not follow the source axis, we include the caveat that our model may be a simplified version of a more complex reality.

The modest densities expected in the IFM allow for two physically motivated constraints. First, we assume that the two core–lobe lengths are intrinsically equal, which implies a bend in the arms unseen because of our viewing angle. This is supported by the jets being ejected far from the host galaxy, and along the minor axis, implying also a lack of interaction with the host. Second, the bend angle, α, is unlikely so extreme as to be greater than 90°. Figure 1 (right) shows a histogram of velocities for galaxies within a 1.5 Mpc from F1. The positive relative velocity means that the galaxy is headed away from the observer. Taken in combination with the fact that the far lobe is more extended with a fainter peak flux, we take the further lobe to be oriented with its jet away from the observer, and the nearer lobe with its jet oriented toward the observer (as in Figure 2).

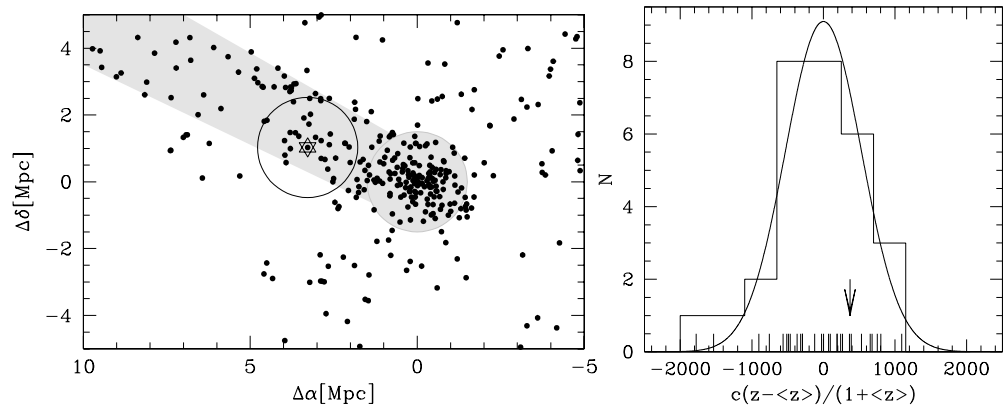

Figure 1. Velocity of F1 with respect to the filament. Left: the spectroscopically confirmed members are shown as black dots, with F1 highlighted as a star. The location of the filament is shaded in gray. The large gray circle marks the cluster R_{500}. The large black circle has a radius of 1.5 Mpc and inscribes the galaxies included in the histogram on the right. Right: an histogram of the velocities of the 29 galaxies relative to their average. It includes galaxies within 1.5 Mpc of F1 and with redshifts between 0.225 and 0.24. The Gaussian corresponds to the normalized distribution of velocities ($\sigma_{\rm los} = 532\,{\rm km\,s^{-1}}$). The vertical lines at the bottom of the histogram mark the relative velocity of each galaxy, F1 is highlighted with an arrow.

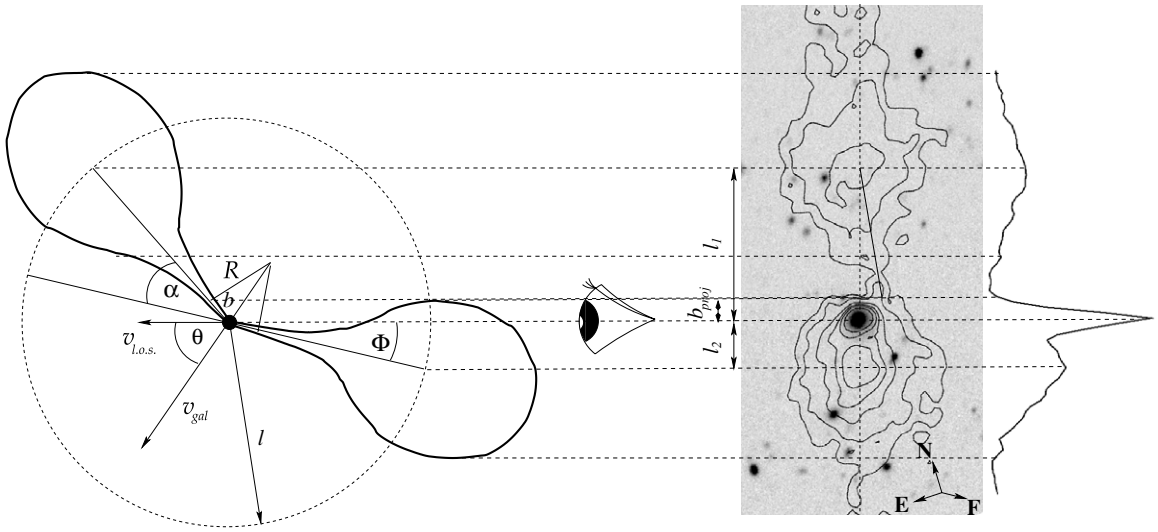

Figure 2. Geometry of the bent DLRS. The *R*-band image surrounding the radio-excess galaxy, F1, is shown in negative gray scale. The black contours show the large lobes of radio emission, the beam is 5 arcsec. The projected core–lobe distances are l_1 and l_2. A cut through the major axis of the radio source is shown at the far right of the image. The large inscribed circle which defines the jet length, l, sets the various angles and projected lengths. The bend angle, α, bend length, b, its projection, $b_{\rm proj}$, and the orientation angle, Φ are as shown. We also show the curvature radius, R, as described in the text. From the galaxy redshift, we can determine the line-of-sight velocity, $v_{\rm l.o.s.}$, which is the line-of-sight component of the true galaxy velocity ($v_{\rm gal}\cos(\theta)$). To highlight how straight the upper jet is, we trace a thin line which joins the upper lobe to the beginning of the bend.

3.1.1. Deducing the Intrinsic Bend

The bottom of Figure 3 shows our model for the bend angle $\alpha = 90^\circ - \arcsin(l_2/l) - \arccos(l_1/l)$, where l is the true core–lobe distance. We take the minimum core–lobe distance to be 171 kpc as measured, and calculate the bend angle as a function of intrinsic jet length. Typical bent DLRSs have jet lengths of under ∼400 kpc (Gower & Hutchings 1984), and a reasonable minimum core–lobe length is ∼250 kpc, so we take $\alpha = 20^\circ$–$30^\circ \sim 25^\circ$. This is consistent with models of Lister et al. (1994) based on a sample of double lobe radio sources in the sky which suggest intrinsic α between 0 and 25°.

3.1.2. Orientation of the Bent DLRS

We calculate the orientation angle of the approaching jet, Φ, as a function of jet length, $\Phi = \arcsin(l_2/l)$. Taking the same range for jet lengths as before, $\Phi \sim 7^\circ$–12° as shown in the middle panel of Figure 3. This is also consistent with the (Lister et al. 1994) models that derive best-fit viewing angles of greater than 50° from the line of sight to the receding jet for their radio galaxies ($180^\circ - \alpha - \Phi = 145^\circ$, in our case).

3.1.3. Jet Curvature

The radius of curvature, R, of the bent DLRS can be calculated as a function of bend angle (and therefore of l). Assuming the jet starts to curve at a length b along the jet, R can be defined as in Figure 3, $R = b/[\cos(180-\alpha)/2]$. Because the jet is essentially straight out to the contours of the lower lobe, we have an observational constraint on the upper limit of the projected component, $b_{\rm proj}$. Therefore the line in the top panel of Figure 3 defines the maximum values of the curvature radius at different l. A minimal value is estimated from the literature as ∼15 kpc (see, for example, O'Donoghue et al. 1993).

3.2. A Probe of the IFM

The presence of a bent DLRS in and of itself suggests an interplay between the radio source and its surroundings. Ram

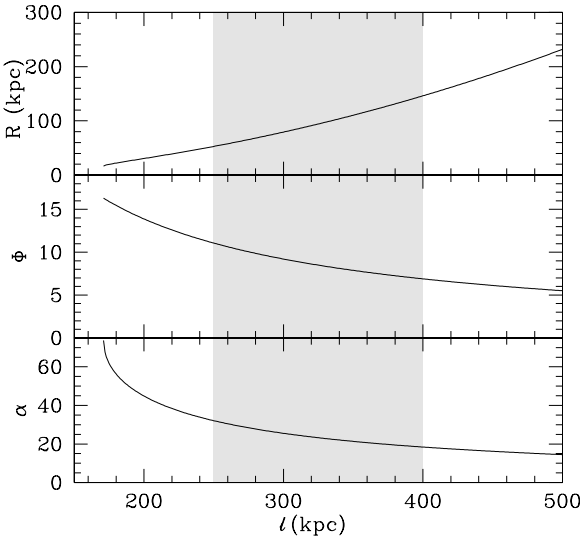

Figure 3. Geometrical models. Top: the radius of curvature, R, as a function of jet length (l). The curve delineates the upper bound of acceptable R, based on the upper limit of the projected bend length, $b_{\rm proj}$. Middle: leading jet orientation (Φ) as a function of jet length. Bottom: bend angle (α) of the jet as a function of l. All angles are defined as in Figure 2. Acceptable values of l include the shaded region with $l = 250$–400 kpc. This range of l defines our constraints on R, Φ, and α.

pressure is likely the cause of the bent morphology, especially in luminous X-ray clusters (Blanton et al. 2001), where the intracluster medium is dense. But it is not clear whether the much less dense IFM could similarly influence the jets.

Presently, we use the source geometry to derive constraints on the density of a posited IFM. In addition, we calculate a merger timescale for the closest companions which is much longer than the lifetime of the jet particles.

3.2.1. Constraints on the Jet Properties and the Intrafilament Medium

We use the Euler equation as in Begelman et al. (1979) and Freeland et al. (2008) to estimate $\rho_{\rm IFM}$:

$$\frac{\rho_{\rm IFM} v^2}{h} = \frac{\omega \Gamma^2 \beta^2}{R}. \quad (1)$$

This model assumes that ram pressure from the relative motion between the source and its surrounding medium causes the bend in the radio jets. We measure the width of the jet, h, as 48 kpc, from our map. Although we point out that this is an upper bound as our 20 cm observations may not resolve the true width of the jet. The term $(\omega\Gamma^2)(\beta^2)$ includes the enthalpy, ω, and depends on the pressure inside the jets and the jet velocity ($\omega = 4P_{\rm min}$). Γ is the relativistic factor, $(1-\beta^2)^{-1/2}$, and $\beta = v/c$. We adopt the same value of $\beta = 0.54 \pm 0.18$ as in Freeland et al. (2008) as it is consistent for speeds of FR I sources with both straight (Arshakian & Longair 2004) and wide angle tail (Jetha et al. 2006) morphologies. R is the radius of curvature and not straightforward to measure, therefore, we calculate our results for several values. The pressure in the jets can be calculated as in Pacholczyk (1970) and Smolčić et al. (2007), and depends on the jet flux density and the spectral index, a:

$$P_{\rm min} = \frac{7}{9}\frac{B_{\rm me}^2}{8\pi}, \quad (2)$$

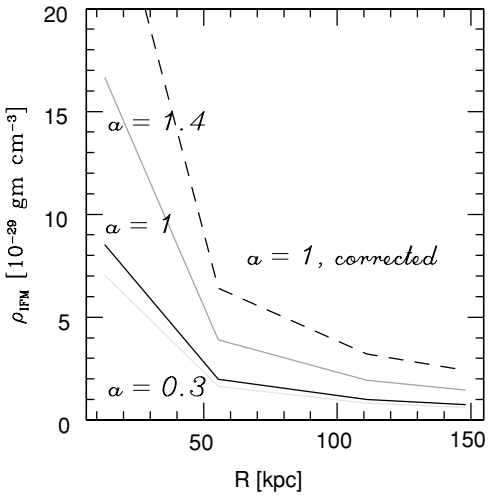

Figure 4. IFM density as a function of curvature radius. The IFM density for several values of spectral index, a are shown as a function of the curvature radius. The dashed line shows the value corrected for relativistic deboosting. The DLRSs in the groups of Freeland et al. (2008) have $R \sim 60$ kpc. Beyond $R \sim 100$ kpc, the $\rho_{\rm IFM}$ begins to stabilize.

where

$$B_{\rm me} = 5.69 \times 10^{-5}\left[\frac{1+k}{\eta}(1+z)^{3+a} \times \frac{1}{\Theta_x \Theta_y l \sin^{3/2}\Phi}\frac{F_o}{\nu_o^a}\frac{\nu_2^{1/2-a} - \nu_1^{1/2-a}}{(1/2)-a}\right]^{2/7}. \quad (3)$$

Radio observations for this source exist only at one frequency, so we cannot measure the spectral index. It is not straightforward to assume a value as there can be wild variability, even within a single source. We therefore calculate the jet power and $\rho_{\rm IFM}$ for several values of a.

We measure a flux density of 0.75 ± 0.26 mJy beam^{-1} in the jet going toward the more distant lobe, $\Theta_x = 6.8$ kpc and $\Theta_y = 4.8$ kpc, and assume cylindrical symmetry in the jet. We calculate the bolometric radio luminosity between frequencies of $\nu_o = 0.01$ and $\nu_1 = 100$ GHz. We set the ratio of relativistic proton to electron energy $k = 1$, as well as 1 for the filling factor, η. We measured an average redshift near F1 of $z = 0.2329$. For $a \sim 1$, $P_{\rm min} = 2 \times 10^{-13}$ dyn cm^{-2}. We do the calculations assuming no relativistic boosting or deboosting, as well as including a factor to account for the effects of deboosting as in Urry & Shafer (1984):

$$L_{\rm boo} = \delta^{2+a} L, \quad (4)$$

where $\delta = [\gamma(1-\beta\cos(\theta))]^{-1}$ and β is defined as above, γ is the Lorentz factor, L is the luminosity at 1.4 GHz and θ is the angle between the line of sight and the velocity vector (see Figure 2). Relativistic deboosting decreases the observed internal jet pressure so the corrected value of $(8 \pm 3.2) \times 10^{-13}$ dyn cm^{-2} is more realistic. The errors are propagated from the measurement errors on the flux density and β.

The source, marked with a star in Figure 1 (left), is traveling mainly orthogonal to the direction of the filament. The filament direction is labeled F in Figure 2. To obtain its velocity relative to the filament, we considered the distribution of velocities relative to the median redshift of the 29 galaxies in the redshift limits of the structure ($z = 0.225$–0.24) and within 1.5 Mpc of F1 (Fadda et al 2008; Edwards et al 2010a). This produces a

$v_{los} = (373 \pm 30)\,\mathrm{km\ s^{-1}}$, highlighted in Figure 1 (right) with an arrow. We deproject by dividing by $\cos(\theta)$, where θ is 90 – (Φ+α/2), obtaining a velocity of $980 \pm 80\,\mathrm{km\ s^{-1}}$.

Figure 4 shows ρ_{IFM} for selected values of the spectral index, a, as a function of R, which begins to stabilize after $R \sim 100$ kpc. The most reasonable choice of a is probably around 1, and the dashed line includes a correction for relativistic deboosting. This gives ρ_{IFM} between (1–20) $\times\ 10^{-29}$ gm cm^{-3}. For $R = 60$ kpc, $\rho_{IFM} = 6.4^{+14.3}_{-5.1} \times 10^{-29}$ gm cm^{-3}.

3.3. Galaxy–Galaxy Mergers Along the Filament

We argue that there has been no significant merger activity that would affect the morphology of the jets. First, the host galaxy of our bent DLRS shows nearly symmetric isophots, and red colors with $(u'–r') = 2.60$, with no clear indications of recent starburst activity in the optical spectrum. Second, although there is a projected close pair only 24 kpc away (SDSS photometric redshift of 0.029), the merger timescale at this distance is significantly longer (∼1 Gyr) than the particle lifetimes in the jet (∼2 Myr).

4. DISCUSSION

Tecce et al. (2010) calculate the ram pressure in rich clusters at $z < 0.5$ to be 2×10^{-11} dyn cm^{-2} and an order of magnitude less for poorer clusters of $M_{vir} \sim 10^{14}\ M_{\odot}$. A1763 is a massive galaxy cluster with central pressures on the order of 2×10^{-10} dyn cm^{-2} and of 10^{-11} dyn cm^{-2} at 1 Mpc from the cluster center (Cavangnolo et al. 2009). At the distance of F1, we infer the minimum jet pressure to be between $(8.0 \pm 3.2) \times 10^{-13}$ dyn cm^{-2} for a= 1, almost 2 orders of magnitude below this. The measured electron density for this cluster at 1 Mpc from the center is 5×10^{-4} cm^{-3}. For reasonable assumptions of the spectral index and for $R = 60$ kpc, we have estimated ρ_{IFM} between $6.4^{+14.3}_{-5.1} \times 10^{-29}$ gm cm^{-3} which gives gas number densities of $6^{+14}_{-5} \times 10^{-5}$ cm^{-3} assuming a mean molecular weight of 0.6.

Direct observations of the X-ray emission in the filament that joins A222 and A223 from Werner et al. (2008) measure the IFM to be 3×10^{-5} cm^{-3}, which agrees with our value to within errors. Although it is possible we are measuring the intragroup medium of an infalling group within the filament, the fact that our values are near to those found in the A222 filament suggest we are indeed measuring the IFM. Our results are also of the same order of magnitude as those of Fang et al. (2010). These authors have calculated the Warm Hot Intergalactic Medium (WHIM) in the Sculptor wall to be 30 times the mean density of the universe, measured by Riordan & Schramm (1991) to be between (2–5) $\times\ 10^{-31}$ gm cm^{-3}. Our results are in agreement with the simulations of Davé et al. (2001) who predict the density of the WHIM to be 4×10^{-6} to 1×10^{-4} cm^{-3}, and consistent with the simulations of Dolag et al. (2006) which predict filament densities ∼10–100 times the mean density (at distances between 2 and 10 Mpc of a massive cluster).

5. CONCLUSIONS

We have found a DLRS 3.4 Mpc from the core of A1763 along the galaxy filament, toward A1770, but well beyond the virial radius of either cluster. Geometrical arguments propel us to surmise an intrinsic bend of $\alpha = 25^{\circ}$ between the jets of F1, seen at $\Phi = 10^{\circ}$ with respect to the line of sight. We have ruled out any significant affect on the radio morphology from either an interaction with the host, or with another galaxy. Bent DLRSs have been found to reside in groups and postulated to exist in filaments (Freeland et al. 2008). Because of our extremely wide field, deep, multiwavelength study of this super structure, we know a priori that the galaxy is ultimately part of the cluster feeding filament. This is the first time such an object has been found so far from the cluster center and identified specifically within a filament. This unique finding has led us to be able to fix observationally motivated constraints on the IFM, which we deduce to be between (1–20) $\times\ 10^{-29}$ gm cm^{-3}. This is consistent with theoretical estimates for filament densities, as well as recent X-ray observations of cluster scale filaments. These observations serve to motivate future measures of the IFM by justifying searches for bent DLRGs in known filaments.

Blanton et al. (2001), starting with a sample of bent DLRSs, find that 80% reside in clusters. We suggest such sources with distances of several Mpc from a rich galaxy cluster center, as markers for rigorous supercluster scale filament searches. We conclude that many of the bent DLRSs found in groups may actually be part of larger scale structures, such as filaments.

We thank the scientific staff at the NRAO, in particular G. Van Moorsel for help with observation planning and F. Owen for help with data reduction techniques. We thank L. Storrie-Lombardi and P. Appleton for fruitful discussions. Support for this work was provided by NASA through an award issued by JPL/Caltech.

This work is based in part on original observations using the Very Large Array operated by the NRAO. The National Radio Astronomy Observatory is a facility of the National Science Foundation operated under cooperative agreement by Associated Universities, Inc.

Facilities: VLA, WIYN (Hydra)

REFERENCES

Arshakian, T. G., & Longair, M. S. 2004, MNRAS, 351, 727
Begelman, M. C., Rees, M. J., & Blandford, R. D. 1979, Nature, 279, 770
Blanton, E. L. 2000, PhD thesis, Columbia Univ.
Blanton, E. L., Gregg, M. D., Helfand, D. J., Becker, R. H., & Leighly, K. M. 2001, AJ, 121, 2915
Carroll, B. W., & Ostlie, D. A. 2006, An Introduction to Modern Astrophysics and Cosmology (New York: Addison-Wesley)
Cavagnolo, K. W., Donahue, M., Voit, G. M., & Sun, M. 2009, ApJS, 182, 12
Croston, J. H. 2008, in ASP Conf. Ser. 386, Extragalactic Jets: Theory and Observation from Radio to Gamma Ray, ed. T. A. Rector & D. S. De Young (San Francisco, CA: ASP), 335
Davé, R., et al. 2001, ApJ, 552, 473
de Vries, W. H., Becker, R. H., & White, R. L. 2006, AJ, 131, 666
Dolag, K., Meneghetti, M., Moscardini, L., Rasia, E., & Bonaldi, A. 2006, MNRAS, 370, 656
Edwards, L. O. V., Fadda, D., Biviano, A., & Marleau, F. R. 2010a, AJ, 139, 434
Edwards, L. O. V., Fadda, D., Frayer, D. T., Lima-Neto, G., & Durret, F. 2010b, AJ, in press (arXiv:1009.5753)
Fadda, D., Biviano, A., Marleau, F. R., Storrie-Lombardi, L. J., & Durret, F. 2008, ApJ, 672, L9
Fanaroff, B. L, & Riley, J. M. 1974, MNRAS, 167, 31
Fang, T., Buote, D. A., Humphrey, P. J., Canizares, C. R., Zappacosta, L., Maiolino, R., Tagliaferri, G., & Gastaldello, F. 2010, ApJ, 714, 1715
Freeland, E., Cardoso, R. F., & Wilcots, E. 2008, ApJ, 685, 858
Gower, A. C., & Hutchings, J. B. 1984, AJ, 89, 1658
Jetha, N. N., Hardcastle, M. J., & Sakelliou, I. 2006, MNRAS, 368, 609
Kundt, W., & Gopal-Krishna, 1980, Nature, 288, 149
Ledlow, M. J., & Owen, F. N. 1996, AJ, 112, 9
Lister, M. L., Hutchings, J. B., & Gower, A. C. 1994, ApJ, 427, 125

O'Donoghue, A. A., Eilek, J. A., & Owen, F. N. 1993, ApJ, 408, 428
Owen, F. N., & Rudnick, L. 1976, ApJ, 205, L1
Pacholczyk, A. G. 1970, Radio Astrophysics. Non-thermal Processes in Galactic and Extragalactic Sources (San Francisco, CA: Freeman)
Rector, T. A., Stocke, J. T., & Ellingson, E. 1995, AJ, 110, 1492
Riordan, M., & Schramm, D. N. 1991, The Shadows of Creation. Dark Matter and the Structure of the Universe (New York: Freeman)
Smolčić, V., et al. 2007, ApJS, 172, 295
Tecce, T. E., Cora, S. A., Tissera, P. B., Abadi, M. G., & Lagos, C. d. P. 2010, MNRAS, 408, 2008
Urry, C. M., & Shafer, R. A. 1984, ApJ, 280, 569
Werner, N., Finoguenov, A., Kaastra, J. S., Simionescu, A., Dietrich, J. P., Vink, J., & Böhringer, H. 2008, A&A, 482, L29
Zirbel, E. L. 1997, ApJ, 476, 489